vigorously for 52 h (23 °C), and the solvent was removed in vacuo. The residual solid was suspended in water (1 mL), the suspension was made basic (pH 9) with the addition of 5% aqueous Na_2CO_3, and the insoluble solid was collected by centrifugation. The residual solid was suspended in water (1 mL), and the suspension was acidified (pH 1) with the addition of 10% aqueous HCl. The insoluble solid was collected by centrifugation and was washed with water (2 × 1 mL). Drying the solid in vacuo afforded **5a** (3.5 mg, 4.0 mg theoretical, 88%) as a gray-brown solid: ^{1}H NMR (Me_2SO-d_6, 200 MHz, ppm) 11.87 (br s, 1 H, NH), 11.63 (br s, 2 H, NH), 11.41 (br s, 1 H, NH), 8.36 (br s, 3 H, C4′, C4″, and C4‴-H), 8.04 (d, 1 H, J = 9 Hz, C4-H), 7.45–7.17 (m, 7 H), 7.02 (s, 1 H), 6.16 (s, 2 H, $CONH_2$), 4.70 (br m, 6 H, C2′, C2″, and C2‴-H), 4.03 (t, 2 H, J = 8 Hz, C2-H), 3.91 (s, 3 H, OCH_3), 3.28–3.54 (br m, 8 H, C1, C1′, C1″, and C1‴ obscured by H_2O); IR (KBr) ν_{max} 3410, 2943, 1701, 1611, 1578, 1507, 1425, 1364, 1343, 1284, 1253, 1210, 1185, 1146, 800, 756 cm^{-1}.

Acknowledgment. We gratefully acknowledge the financial support of the National Institutes of Health (CA 41986), the Alfred P. Sloan Foundation, and Purdue University for administration of a David Ross Fellowship (RSC).

Structure and Conformation of Halomycin B in Solid State and Solution

S. K. Arora* and A. M. Kook

Drug Dynamics Institute, College of Pharmacy, University of Texas, Austin, Texas 78712-1074

Received October 17, 1985

Structural studies have been carried out on halomycin B ($C_{43}H_{58}N_2O_{12}$), an ansamycin antibiotic, to study the effect of the substitution at the 4-position of the naphthohydroquinone on the conformation of the ansa chain. The antibiotic crystallizes as monohydrate ethyl acetate solvate in the monoclinic space group $P2_1$, with the following cell dimensions: a = 12.362 (1), b = 12.846 (2), c = 16.160 (2) Å; β = 107.7 (1)°; Z = 2; D_{measd} = 1.24 g cm^{-3}. The structure was solved by repeated use of direct methods and Fourier synthesis and refined to the final R value of 0.052 for 3741 reflections. The conformation revealed indicates that, contrary to previous assumptions, the substitution at the C(4) position (substituted pyrrolidine, in this case) may affect the conformation of the middle part of the ansa chain, thus making halomycin B less active against the enzyme DNA-dependent RNA polymerase (DDRP). There is a trapped water molecule between the chromophore and the ansa chain. This water molecule is involved in hydrogen bonding with the O(10) of the ansa chain, the O(12) of the substituted pyrrolidine, and an oxygen of ethyl acetate. The NMR studies indicate that two isomers exist in chloroform solution. The major isomer (80%) has a conformation that is similar to that observed in solid state. The dynamic process involved in the interconversion of these two isomers is shown.

Halomycins that contain a substituted pyrrolidine ring at the C(4) position of rifamycin SV belong to a well-known class of antibiotics called ansamycins. Halomycins A, B, and C differ from each other in their hydroxylation pattern in the ansa chain or pyrrolidine moiety (Figure 1). They are produced by *Micromonospora halophytica*[1] and are highly active against gram-positive bacteria. In general, rifamycins are used for the treatment of tuberculosis and have some antitumor activity.

A number of studies have been done both in solid state[2-6] and in solution to correlate the conformation of the ansa chain and the biological activity of rifamycins. Attempts have also been made to study the effects of 3-substitution on the conformation of the ansa chain. Rifampicin, which is highly active, is a 3-substituted rifamycin SV. The present study has been carried out to study the molecular structure and conformation of halomycin B as well as the effect of 4-substitution on the conformation of the ansa chain and thus its biological activity.

Table I. Crystal Data for Halomycin B

$C_{43}H_{58}N_2O_{12}\cdot H_2O\cdot EtOAc$	V = 2444.4 Å^3
M_r 900.3	Z = 2
monoclinic, $P2_1$	D_{measd} = 1.24 g·cm^{-3}
a = 12.362 (1) Å	D_{calcd} = 1.23 g·cm^{-3}
b = 12.846 (2) Å	temp = −110 °C
c = 16.160 (2) Å	radiation, Mo Kα (λ = 0.710 69 Å)
β = 107.7 (1)°	$(\sin\theta)/\lambda_{max}$ = 0.62 Å^{-1}

Experimental Section

X-ray. Halomycin B was supplied by Dr. A. Ganguly of Scherring Corp. Yellow needle-shaped crystals were grown from a mixture of ethyl acetate and benzene after many unsuccessful attempts. The crystal data are given in Table I. Intensities of 5297 reflections, $4.0 \le 2\theta \le 53.0°$, were measured by use of Mo Kα radiation (λ = 0.710 69 Å) on a Syntex $P2_1$ diffractometer equipped with a graphite monochromator and a Syntex LT-1 inert gas (N_2) low-temperature delivery system, using the ω scan technique, a variable scan rate (2.0–6.0°), and a scan range of 2.0° with a scan to background ratio of 1. A total of 3741 reflections greater than $3\sigma(I)$ was considered observed. The intensities were corrected for Lorentz and polarization effects, but no absorption correction was applied.

After numerous unsuccessful attempts, a partial structure (16 atoms corresponding to the two fused six-membered rings and few substituents) was obtained by the direct-methods program MULTAN.[7] The complete structure (all non-hydrogen atoms) was obtained by the repeated use of the Fourier and difference Fourier

(1) Weinstein, M. J.; Leudemann, A. M.; Oden, E. M.; Wagman, G. H. *Antimicrob. Agents Chemother.* **1967**, 435–441.
(2) Brufani, M.; Cerrini, S.; Fideli, W.; Vaciago, A. *J. Mol. Biol.* **1974**, *87*, 409–435.
(3) Lancini, A.; Zanichelli, W. *Structure Activity Relationship among Semisynthetic Antibiotics*, Perlman, R., Ed.; Academic: New York, 1977; pp 531–600.
(4) Arora, S. K. *Acta Crystallogr., Sect. B: Struct. Crystallogr. Cryst. Chem.* **1981**, *B37*, 152–159.
(5) Arora, S. K. *Mol. Pharmacol.* **1983**, *23*, 133–140.
(6) Arora, S. K. *J. Med. Chem.* **1985**, *28*, 1099–1102.
(7) Germain, G.; Main, P.; Wollfson, M. M. *Acta Crystallogr., Sect. A: Cryst. Phys., Diffr., Theor. Gen. Crystallogr.* **1971**, *A27*, 368–376.

0022-3263/87/1952-1530$01.50/0

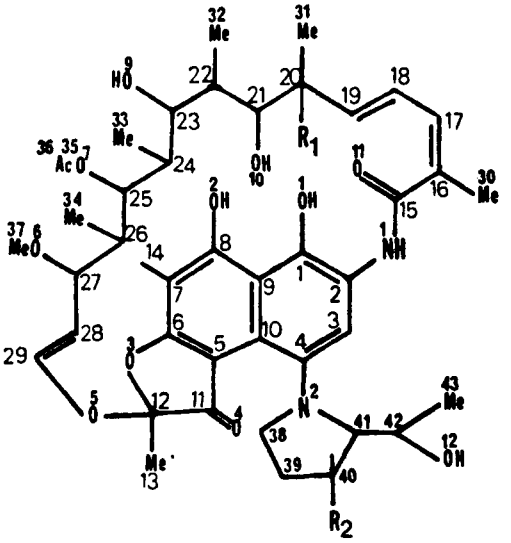

HALOMYCINS	R_1	R_2
A	H	OH
B	H	H
C	OH	H

Figure 1. Chemical formulas for halomycins A, B, and C.

maps. The initial R factor, with all the non-hydrogen atoms in, was 0.38. Refinement of the positional and isotropic thermal parameters for non-hydrogen atoms reduced the R value to 0.19 and 3741 reflections. The anisotropic refinement reduced the R value to 0.11. At this stage, all the hydrogen atoms of halomycin B as well as water and ethyl acetate molecules were located, and the structure was refined by use of anisotropic thermal parameters for non-hydrogen atoms and isotropic thermal parameters for hydrogen atoms to a final R of 0.052. The refinement was based on F_o with unit weights, the quantity minimized being $\Sigma(F_o - F_c)^2$. The scattering factors used were those of Cromer and Mann.[8] The final atomic coordinates and their standard deviations are given in Table II.

NMR. The ^1H spectra were obtained on a 4.90 mM solution of halomycin B in $CDCl_3$ at 200.1 MHz on Nicolet 200, 361.1 MHz on Nicolet 360, and 500.1 MHz on GN-500 NMR spectrometers equipped with variable-temperature thermocouple devices. Typically, 32–32K fids were obtained in 1.6, 2.22, and 4.1 s with spectral windows of 4014, 7220, and 10 002 Hz (20.0 ppm) and pulse widths of 2, 4.5, and 5 μs (flip angle 44°). The spectra were obtained by means of quadrature phase detection and computer alternating pulse phases with a recycle delay of 1.0 s. The final spectrum was weighted by use of a 0.04-Hz line broadening and zero-filled to 64K, which results in a final digital resolution of 4.08, 2.25, and 1.64 Hz, respectively.

The two-dimensional COSY experiment was obtained with a modified $(90°x–t_1–60°x–\text{Acq})_n$ pulse sequence that emphasizes cross peaks.[9] Typically, 32–1K fids were obtained for each of $256 - t_1$ increments with a spectral window in both dimensions of 4000 Hz, which was obtained in 0.256 s with recycle delay of 2 s. The spectra were sine-bell weighted in the second dimension and zero-filling and Gaussian sine-belled in the first dimension to obtain a final data point array of 512 × 512.

The ^1H NOE difference spectra were obtained at 500 MHz with a 3-s decoupler irradiation time at 0.5 W of power, which generated an effective bandwidth of 10 Hz. A 3-s recycle time was used between pulses to regenerate a sufficient steady-state spin population. On average, 350 32K fids were obtained for each irradiation of the five methyl doublets (–0.7 to +1.5 ppm), proton 25 (4.88 ppm), and proton 3 (8.68 ppm) with a 1-Hz line broadening factor to minimize artifacts inherent in the experiment.

(8) Cromer, D.; Mann, B. *Acta Crystallogr., Sect. A: Cryst. Phys., Diffr., Theor. Gen. Crystallogr.* **1968**, *A24*, 321–324.
(9) Bax, A. *Two-Dimensional NMR of Liquids*; Delft: Holland, 1982.

Table II. Positional Parameters and U_{eq} for Halomycin B

atom	x	y	z	u
O(W)	0.6531 (5)	0.190725	0.2089 (4)	0.073 (3)
O(1)	0.7209 (4)	0.0293 (4)	0.5851 (3)	0.0340 (14)
O(2)	0.6986 (4)	–0.1381 (3)	0.5086 (3)	0.0352 (15)
O(3)	0.4585 (3)	–0.1694 (3)	0.2214 (2)	0.0290 (12)
O(4)	0.3238 (3)	0.0770 (3)	0.1759 (2)	0.0336 (13)
O(5)	0.3993 (3)	–0.933 (3)	0.0833 (2)	0.0267 (12)
O(6)	0.5949 (3)	0.0989 (3)	–0.582 (3)	0.0373 (15)
O(7)	0.8401 (3)	–0.1938 (3)	0.0323 (2)	0.0357 (14)
O(8)	0.7784 (4)	–0.3193 (3)	0.1048 (3)	0.046 (2)
O(9)	0.7543 (3)	–0.1642 (3)	0.2325 (3)	0.0358 (14)
O(10)	0.7546 (3)	0.0220 (4)	0.3135 (3)	0.0373 (4)
O(11)	0.7656 (3)	0.3752 (4)	0.6583 (2)	0.043 (2)
O(12)	0.4543 (6)	0.2952 (6)	0.1815 (4)	0.050 (2)
N(1)	0.6658 (4)	0.2344 (4)	0.5933 (3)	0.031 (2)
N(2)	0.3718 (3)	0.2008 (3)	0.3110 (3)	0.0236 (14)
C(1)	0.6395 (4)	0.0682 (5)	0.5172 (3)	0.029 (2)
C(2)	0.6075 (4)	0.1721 (4)	0.5211 (3)	0.026 (2)
C(3)	0.5187 (4)	0.2130 (4)	0.4531 (3)	0.023 (2)
C(4)	0.4699 (4)	0.1564 (4)	0.3796 (3)	0.024 (2)
C(5)	0.4619 (4)	–0.0130 (4)	0.2947 (3)	0.023 (2)
C(6)	0.5035 (4)	–0.1157 (4)	0.2967 (3)	0.026 (2)
C(7)	0.5809 (4)	–0.1623 (4)	0.3665 (3)	0.027 (2)
C(8)	0.6256 (4)	–0.1005 (4)	0.4406 (3)	0.027 (2)
C(9)	0.5887 (4)	0.0081 (4)	0.4422 (3)	0.022 (2)
C(10)	0.5039 (4)	0.0525 (4)	0.3700 (3)	0.020 (2)
C11	0.3821 (4)	0.0004 (4)	0.2115 (3)	0.024 (2)
C12	0.3744 (4)	–0.1031 (4)	0.1621 (3)	0.028 (2)
C(13)	0.2594 (5)	–0.1539 (5)	0.1413 (4)	0.036 (2)
C(14)	0.6161 (5)	–0.2751 (5)	0.3654 (4)	0.038 (2)
C(15)	0.7178 (4)	0.3277 (5)	0.5910 (3)	0.030 (2)
C(16)	0.7164 (4)	0.3726 (4)	0.5048 (3)	0.026 (2)
C(17)	0.7690 (4)	0.3264 (4)	0.4534 (3)	0.025 (2)
C(18)	0.8237 (4)	0.2251 (4)	0.4650 (3)	0.027 (2)
C(19)	0.8736 (4)	0.1869 (4)	0.4099 (3)	0.028 (2)
C(20)	0.9279 (4)	0.0820 (5)	0.4145 (4)	0.031 (2)
C(21)	0.8752 (4)	0.0251 (4)	0.3277 (3)	0.026 (2)
C(22)	0.9252 (5)	–0.0822 (4)	0.3203 (3)	0.030 (2)
C(23)	0.8655 (4)	–0.1356 (4)	0.2315 (3)	0.029 (2)
C(24)	0.8606 (4)	–0.0674 (5)	0.1519 (4)	0.032 (2)
C(25)	0.7810 (4)	–0.1135 (4)	0.0675 (3)	0.027 (2)
C(26)	0.7285 (4)	–0.0382 (4)	–0.0082 (3)	0.026 (2)
C(27)	0.6335 (4)	0.0258 (4)	0.0116 (3)	0.026 (2)
C(28)	0.5374 (4)	–0.0415 (4)	0.0181 (3)	0.026 (2)
C(29)	0.4954 (4)	–0.0370 (4)	0.0836 (3)	0.027 (2)
C(30)	0.6612 (5)	0.04782 (5)	0.4841 (4)	0.036 (2)
C(31)	1.0572 (5)	0.0944 (6)	0.4337 (5)	0.048 (2)
C(32)	0.9238 (6)	–0.1558 (6)	0.3946 (4)	0.042 (2)
C(33)	0.9846 (5)	–0.0488 (7)	0.1493 (4)	0.051 (3)
C(34)	0.8120 (5)	0.0320 (6)	–0.0352 (4)	0.040 (2)
C(35)	0.8275 (5)	–0.2927 (5)	0.0537 (4)	0.038 (2)
C(36)	0.8833 (6)	–0.3661 (6)	0.0072 (5)	0.056 (3)
C(37)	0.5127 (6)	0.1695 (6)	–0.0463 (5)	0.055 (3)
C(38)	0.2594 (5)	0.1818 (5)	0.3282 (4)	0.034 (2)
C(39)	0.1777 (6)	0.2560 (7)	0.2636 (5)	0.055 (3)
C(40)	0.2527 (6)	0.3342 (6)	0.2349 (4)	0.045 (2)
C(41)	0.3721 (5)	0.3174 (4)	0.2956 (3)	0.032 (2)
C(42)	0.4696 (6)	0.3461 (5)	0.2611 (4)	0.042 (2)
C(43)	0.4713 (8)	0.4664 (6)	0.2494 (5)	0.072 (3)
O(1′)	0.8158 (9)	0.3637 (8)	0.2378 (5)	0.150 (50)
O(2′)	0.9431 (7)	0.4543 (6)	0.1956 (5)	0.111 (4)
C(1′)	0.8421 (13)	0.3221 (12)	0.1038 (7)	0.150 (8)
C(2′)	0.8626 (11)	0.3822 (9)	0.1837 (6)	0.096 (5)
C(3′)	0.949 (2)	0.520 (2)	0.2851 (13)	0.243 (15)
C(4′)	1.0431 (15)	0.5886 (14)	0.2591 (9)	0.245 (12)

Results and Discussion

The bond distances and angles in the molecule agree fairly well with those observed in rifamycin S and rifamycin SV. The bond distances and angles in the pyrrolidine moiety are normal. Figure 2 depicts the stereochemistry of the molecule. The least-squares plane of the five-membered ring, consisting of C(5), C(6), C(11), C(12), and O(3), makes a dihedral angle of 1.3° with the plane of the naphthohydroquinone ring. A least-squares plane through the 17 atoms of the ansa chain makes an angle of

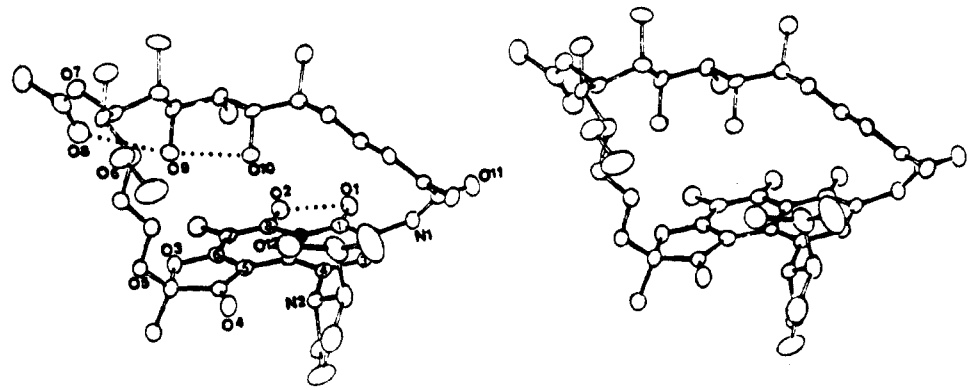

Figure 2. Stereoview of halomycin B, also showing some hydrogen bonds.

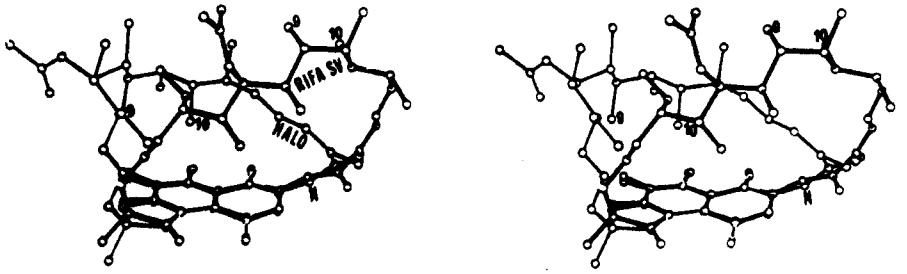

Figure 3. Comparison of the conformation of halomycin B with that of rifamycin SV. The pyrrolidine part has been omitted for the sake of clarity.

Table III. Torsion Angles (deg) along the Skeleton of the Ansa Chain in Rifamycin S, Rifamycin SV Carbomethoxyrifamycin S, Rifamycin B, Rifampcin, Halomycin B, Rifamycin S, Iminomethyl Ether, Tolypomycinone, and Rifamycin Y

	RIF S[6]	RIF SV[5]	CMR S[13]	RIF B[2]	RIFAMP[14]	HALO	RIF IMP[4]	TOLY[15]	RIF Y[2]
C(1)–C(2)–N–C(15)	166	167	−141	−32	−55	125	−132	−171	−26
C(2)–N–C(15)–C(16)	−164	−171	177	180	179	0	17	179	−168
N–C(15)–C(16)–C(17)	133	119	63	−43	−31	−65	50	80	−47
C(15)–C(16)–C(17)–C(18)	−3	−3	2	5	4	7	4	−2	−8
C(16)–C(17)–C(18)–C(19)	−173	−173	169	168	155	−180	−174	−152	180
C(17)–C(18)–C(19)–C(20)	176	−179	−179	−175	−165	−180	174	122	171
C(18)–C(19)–C(20)–C(21)	−60	−52	−30	−11	−19	126	−120	0	111
C(19)–C(20)–C(21)–C(22)	−177	176	180	170	169	178	−173	170	−76
C(20)–C(21)–C(22)–C(23)	−170	−175	−178	−179	−176	179	175	−170	−84
C(21)–C(22)–C(23)–C(24)	65	62	57	53	62	52	−60	68	143
C(22)–C(23)–C(24)–C(25)	−169	180	−174	174	165	−168	170	173	180
C(23)–C(24)–C(25)–C(26)	173	176	169	155	u59	155	−140	−175	159
C(24)–C(25)–C(26)–C(27)	−165	174	180	174	153	−75	72	178	151
C(25)–C(26)–C(27)–C(28)	−166	−179	180	−170	−171	−63	72	67	−174
C(26)–C(27)–C(28)–C(29)	−113	−101	−110	117	118	−130	−119	123	113
C(27)–C(28)–C(29)–O(5)	−180	−179	−176	168	−175	170	−178	175	−176
C(28)–C(29)–O(5)–C(12)	−136	−118	−127	49	65	169	163	42	78
C(29)–O(5)–C(12)–O(3)	−64	−58	−52	−79	−78	−69	71	−70	−84

41° with the chromophore. The configuration in the pyrrolidine ring is 2*R*,3*S*, which is the same as that predicted by Ganguly et al.[10] The torsion angles around the five-membered pyrrolidine ring, starting with the N(2)–C(38) bond and going in the clockwise direction, are 48.9, −16.8, −10.8, 34.1, and −45.0°. By Altona and Sundaralingam's method[11] for conformational analysis of the five-membered rings as well as the above torsion angles, the calculated value of *P* (phase angle of pseudorotation) is 1.1°. This indicates a twist-type N or C(39) endo conformation for the pyrrolidine ring. The dihedral angle between the least-squares plane through atoms of the pyrrolidine ring and through those of the naphthohydroquinone ring has a value of 69.1°.

Brufani et al.[2] had suggested that the substitution at the 3- or 4-position of the chromophore should not affect the conformation of the middle part of the ansa chain and thus should not reduce the activity of the antibiotic against the enzyme DNA-dependent RNA polymerase. Such is not the case in halomycin B (Figure 3). The C(4)-attached substituted pyrrolidine ring does alter the conformation of the ansa chain in such a way that the spatial arrangement of oxygens O(9) and O(10) is altered, making the conformation of the ansa chain similar to that observed in less active rifamycins. Table III compares the torsion angles along the ansa chain of various rifamycins. Comparing the torsion angles in halomycin B and rifamycin SV,[5] the first major difference starts at C(2)–N–C(15)–C(16), where the values are −171 and 0°, indicating a rotation around the N–C(15) direction. The second major difference shows up in angle C(18)–C(19)–C(20)–C(21) (−52 and +126°), indicating that the orientation of C(21) and thus of O(10) with respect to the chromophore has changed, i.e., O(10) which is one of the oxygens important for biological activity against DDRP is directed toward the plane of the chromophore rather than parallel to it. This also causes a change in the orientation of the C(23)–O(9) bond and

(10) Ganguly, A. K.; Szmulewicz, S.; Sarve, O. Z.; Greeves, D.; Morton, J.; McGlotten, J. *J. Chem. Soc., Chem. Commun.* **1974**, 395–396.
(11) Altona, C.; Sundaralingam, M. *J. Am. Chem. Soc.* **1972**, *94*, 8205–8212.

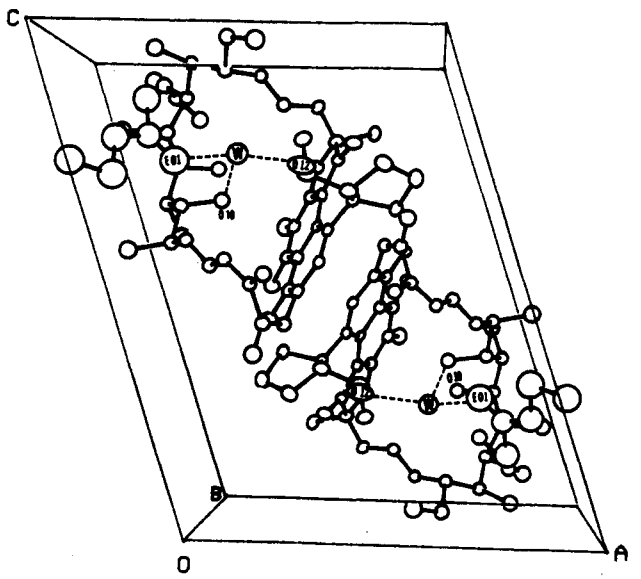

Figure 4. Packing of the molecules in the unit cell. Hydrogen bonding involving water oxygen has also been depicted.

Table IV. Hydrogen Bond Distances

donor	acceptor	D, Å	proton	acceptor	D, Å
O(1)	O(2)	2.46	HO(1)	O(2)	1.79
O(9)	O(8)	2.95	HO(2)	O(1)	1.82
O(10)	O(9)	2.73	HO(9)	O(8)	2.22
O(12)	O(W)	2.72	HO(10)	O(9)	1.95
O(W)	O(10)	2.80	HO(12)	O(W)	1.89
O(W)	O(1′)	2.94	H(10) (W)	O(1)	2.02
			H(20) (W)	O(1′)	2.12

the acetyl group at C(25).

Cellai et al.[12] did a comparative study on the conformation of some rifamycins in solid state and in solution and observed that four kinds of isomers exist. These are generated by the combination of two rotations: one relative to the amidic plane and the other relative to the plane containing the C(28)=C(29) double bond. Thus, the differences observed at the junction of C(2) and C(28) are attributable to different isomers existing in rifamycins, but the difference in the conformation of the middle part of the ansa chain is surprising.

In the case of rifamycin B *p*-iodoanilide, the 4-substitution did not alter the conformation of the middle part of the ansa chain. But the results in the case of halomycin B are different. Thus, it seems that whether or not a 4-substitution will have an effect on the conformation of the ansa chain will depend upon the kind of substituents it has. If the substituent is a proton donor, e.g., a hydroxyl group, it can form a hydrogen-bonding network involving O(10) and water oxygen, thus disturbing the conformation of the middle part of the ansa chain. This will disturb the spatial arrangements of O(9) and O(10), which are important for biological activity against DNA-dependent RNA polymerase. In the present case, the trapped water molecule forms the bridge between O(12), O(10), and O(1′) of ethyl acetate. Figure 4 shows the packing of the molecules in the unit cell as well as the hydrogen bonding involving the water molecule. Table IV gives H bond distances.

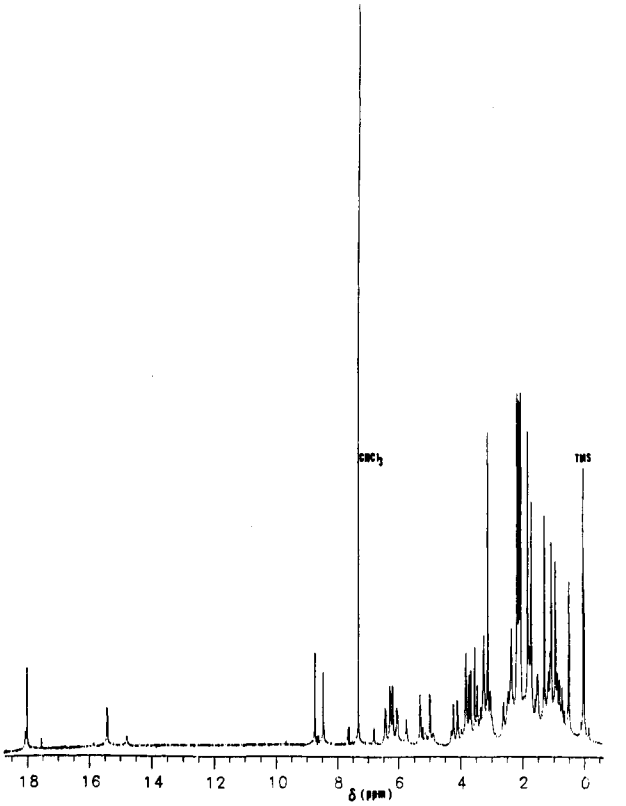

Figure 5. ^{1}H NMR (500-MHz) spectrum in $CDCl_3$.

High-resolution NMR studies were conducted to assign the proton resonances in halomycin B and also to compare the conformation of the antibiotic in solid state and solution. When a 200-MHz spectrum in $CDCl_3$ was examined, signals appeared around 15 and 18 ppm that had not been observed (or not reported) by Cellai et al.[12] in their NMR investigations of various rifamycins and their derivatives. A 360-MHz spectrum confirmed that these peaks were not spurious. It was also observed (as had been reported by Cellai et al.[12]) that two conformers exist in $CDCl_3$. The ratio of major to minor isomer is approximately 4:1 at room temperature.

Figure 5 shows the proton (500-MHz) spectrum. All the resonance lines corresponding to the major isomer and some to the minor isomer have been assigned. The assignments were made with the help of NMR studies on rifamycins S and SV (Cellai et al.[12]) and COSY connectivities. Table V gives the chemical shifts for halomycin B and compares it with chemical shifts for rifamycins SV and S. Due to the presence of the two slowly exchanging conformations in $CDCl_3$, only the assignments of the major isomer and its chemical shifts and J coupling constants (greater than 6 Hz) in the one-dimensional spectrum can be obtained. Selected chemical shifts for the minor isomer are also reported where overlap of the chemical shifts are not severe. Most of the assignments were obtained from the analysis of the cross peak connectivity of the J-coupled spin systems.

Figure 6 shows the 2D COSY spectrum of halomycin B. It is apparent that, due to chemical exchange and the stereochemistry around the ansa chain, the cross peak from protons that have dihedral angles between 65 and 100° and small ^3J(H–H) coupling constants are not clearly observed. Therefore, proton shift assignments were based upon 1- and 2D NOE spectra, Shoolrey chemical shift calculations,

(12) Cellai, L.; Cerrini, S.; Segre, A.; Brufani, M.; Fideli, W.; Vaciago, A. *J. Org. Chem.* **1982**, *47*, 2652–2661.
(13) Brufani, M.; Cellai, L.; Cerrini, S.; Fideli, W.; Segree, A.; Vaciago, A. *Mol. Pharmacol.* **1982**, *21*, 394–399.
(14) Gadret, M.; Gourselle, M.; Liger, J. M.; Colleter, J. C. *Acta Crystallogr., Sect. B: Struct. Crystallogr. Cryst. Chem.* **1975**, *B31*, 1454–1462.
(15) Brufani, M.; Cellai, L.; Cerrini, S.; Fideli, W.; Vaciago, A. *Mol. Pharmacol.* **1978**, *14*, 693–703.

Table V. Chemical Shifts for Halomycin B (for Numbering See Figure 1) in $CDCl_3$ Compared with Chemical Shifts in Rifamycin S, Rifamycin SV, and Halomycin B Fragments

RIF S	RIF SV	HALO B[c]	HALO B[b]	HALO B[a]		HALO B[a]	HALO B[b]	HALO B[c]	RIF SV	RIF S
8.5	7.9		6.75	8.68	HC^{3}					
			7.61	8.41	HN^{1}					
					$C^{15}{=}O$					
					$C^{16}CH_3{}^{30}$	2.14			2.05	2.02
6.25	6.2	6.22	5.10	6.24	HC^{17}					
6.31	6.3	6.54	5.70	6.38	HC^{18}					
5.93	5.75	6.12	5.06	5.99	HC^{19}					
2.27	2.30			2.42	$HC^{20}CH_3{}^{31}$	0.91	0.64		0.8	0.82
3.55	3.60			3.77	$HC^{21}OH^{10}$	3.75				3.70
1.78				1.77	$HC^{22}CH_3{}^{32}$	1.04	0.83		1.0	1.00
2.98	3.0			2.98	$HC^{23}Oh^{9}$	3.66				3.65
1.96				1.45	$HC^{24}CH_3{}^{33}$	0.46	0.83		0.65	0.65
4.60	4.9	4.92		4.83	$HC^{25}OAc^{36}$	2.12		1.82		2.02
1.5				1.48	$HC^{26}CH_3{}^{34}$	−0.03	1.05		−0.1	0.20
3.37	3.5			3.41	$HC^{27}OCH_3{}^{37}$	3.07	3.21	3.02	3.05	3.10
5.06	5.0	4.92	5.08	5.24	HC^{28}					
6.20	6.15	5.96	6.08	6.15	HC^{29}		trapped H_2O molecule at 1.60 ppm			
12.5			17.94	18.0	OH^{1}					
			14.75	15.4	OH^{2}					
				3.49	OH^{12}					
1.72	1.80			1.80	$CH_3{}^{13}$					
2.33	2.1			2.00	$CH_3{}^{14}$					
		3.26		3.75	$CH_2{}^{38}$					
				3.20	$CH_2{}^{39}$					
			2.33	2.55	$CH_2{}^{40}$					
		3.88		4.05	HC^{41}					
				4.18	HC^{42}					
				1.26	$CH_3{}^{43}$					

[a] Major isomer. [b] Minor isomer. [c] NMR study by Ganguly[10] on fragments of halomycin B. The partial assignments were based on NOE difference spectra.

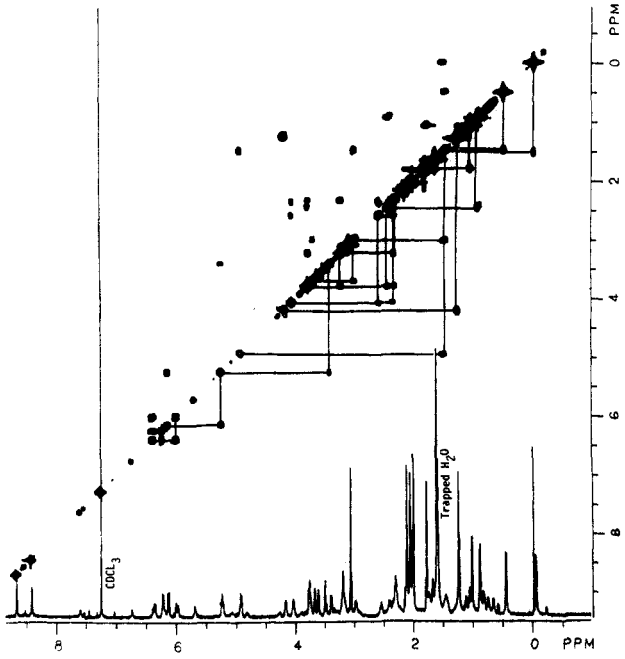

Figure 6. Contour plot of the COSY spectrum.

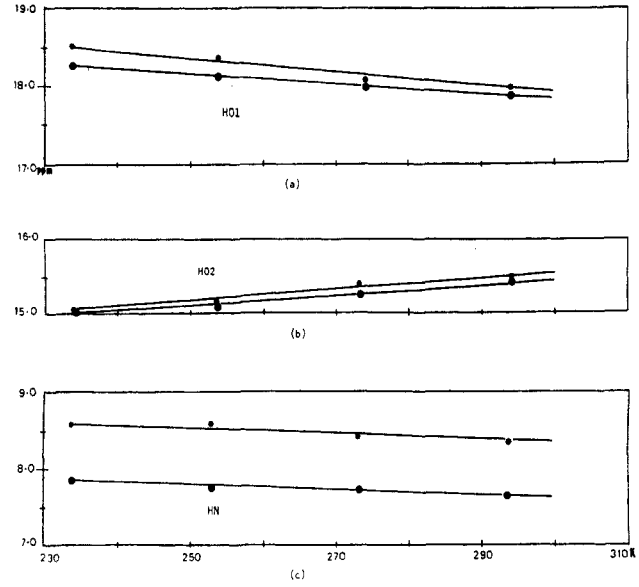

Figure 7. Temperature variation of chemical shifts of major (*) and minor (●) isomers: (a) HO(1), (b) HO(2), (c) HN. The temperatures studied were 0, −20, −40, and −60 °C.

and previous assignments of halomycin B. Wherever possible, COSY cross peak connectivity is shown on contour plot.

The results of the 1- and 2D NOE work indicate that both the exchange and through-space effects are present in this molecule at room temperature at the very slow-exchange limit. The 1-NOE difference experiments were obtained under conditions that emphasize chemical exchange. This did not detract from the observation of through-space interactions, which were also observed. As a matter of fact, the phase of the cross peak helped to distinguish these phenomena (exchange showed negative peaks and NOE peaks were positive).

Examination of the NOE difference spectra of the upfield methyl doublets along the ansa chain (not shown) aided us in the assignment of the protons along the chain. It is apparent from the COSY spectrum that vicinal protons along the ansa chain show (in many cases) very small couplings and cannot be assigned. Using the NOE (through space) interaction, we can correct this discontinuity and get some 3D distance (conformation) information.

Upon irradiation of methyl peak H(34) (−0.03 ppm), we observed an exchange peak with a methyl doublet (1.05 ppm) of the minor tautomer. In addition, there was a very strong cross peak (3%) to proton H(26) (1.48 ppm, a vicinal methine) and smaller (1%) NOE's to methyl H(33) (0.46

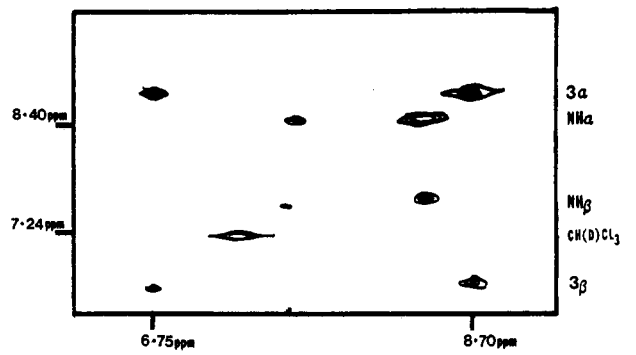

Figure 8. Expansion of the 2D NOESY spectrum of amide and aromatic protons.

ppm) and protons H(25) (4.83 ppm), H(28) (5.24 ppm), and H(27) (3.41 ppm). Irradiation at H(3) (8.68 ppm) gave a strong exchange cross peak at H(3) (6.75 ppm), which rechecks the 2D NOESY spectrum (Figure 8) results.

The variability of chemical shifts from those observed in rifamycins S and SV is low for most of the functional groups except H(24) (0.49 ppm), H(3) (0.79 ppm), HO(1), and HO(2). The change in chemical shift for the H(3) proton from rifamycin SV is probably due to the pyrrolidine substitution at C(4). The position for the amide proton in the major isomer is similar to that observed in other rifamycins. At low temperature, the signals of major and minor isomers start to coalesce. Figure 7 depicts the variability of chemical shifts for HN and H'N (minor isomer) protons at different temperatures. The resonance for the H(18) proton (6.38 ppm) is very close to that reported for rifampicin (6.55 ppm).[12] There is not second resonance in the 6.7–7.2 ppm range as had been suggested by Cellai et al.[12] The difference in the H(24) chemical shift indicates that the middle part of the ansa chain in halomycin B may have a different conformation than that of rifamycin SV. Chemical shifts for H(26)–H(29) protons are similar to those in rifamycin SV. The H(18) proton has a chemical shift of 6.38 ppm for the major isomer. This is close to the value found in rifampicin (6.55 ppm).

The signals at 15.4 and 18.0 ppm were assigned to HO(1) and HO(2) protons. To check whether these and other hydroxyl assignments were correct, a D_2O exchange experiment was conducted; all the hydroxyl signals HO(1) (18.0, 17.74), HO(2) (15.4, 14.75), HO(9) (2.31, HO(10) (3.66), and HO(12) (3.49) disappeared. It is interesting to note that (in preliminary work) the addition of D_2O to the halomycin B solution slows the elimination of (3–3.5 ppm) hydroxylic protons along the ansa chain and a subsequent shift of the trapped H_2O peak at 1.60–4.8 ppm. This shifting showed a changing of the coupling patterns of some of the aliphatic and olefinic protons along the ansa chain. This may indicate, in fact, it may be the trapped H_2O molecule that helps to maintain the major tautomeric

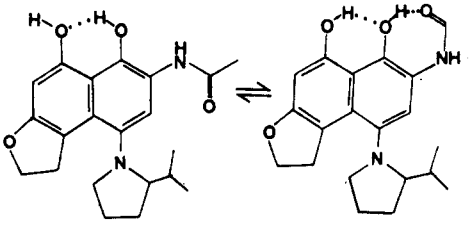

Figure 9. Slow exchange process.

Table VI. Comparison of the Selected Dihedral Angle Values Obtained by ^1H NMR and X-rays for Halomycin B

dihedral angle	J,[a] Hz	angle values, deg NMR	X-ray
H(17)–C(17)–C(18)–H(18)	10.0	150	−174
H(18)–C(18)–C(19)–H(19)	15.3	165	−171
H(18)–C(19)–C(20)–H(20)	6.1	135	−165
H(20)–C(20)–C(21)–H(21)	8.1	160	178
H(21)–C(21)–C(22)–H(22)			166
H(22)–C(22)–C(23)–H(23)			−60
H(23)–C(23)–C(24)–H(24)			−86
H(24)–C(24)–C(25)–H(25)			−169
H(25)–C(25)–C(26)–H(26)	10.7	25	−65
H(26)–C(26)–C(27)–H(27)	6.6	145	171
H(27)–C(27)–C(28)–H(28)	7.5	147	−170
H(28)–C(28)–C(29)–H(29)	12.2	156	178
H(38)–C(38)–C(39)–H(39)	8.4	10	−13
H(39)–C(39)–C(40)–H(41)	6.7	148	119
H(42)–C(42)–C(43)–H(43)	6.8	147	156

[a] NMR coupling constants (J) from which dihedral angles were calculated.

structure of halomycin B in $CDCl_3$. The two signals each for HO(1) and HO(2) indicate a slow exchange process of the type shown in Figure 9. The effect of temperature on the chemical shifts of HO(1) and HO(2) is shown in Figure 8. The chemical shifts move downfield for HO(2) (18.0–18.5 ppm) and upfield for HO(1) (15.4–15.0 ppm). Figure 8 shows the 2D NOESY spectrum in the 7–9 ppm range and the assignment of HN(1) and H(3) protons.

Because of the presence of two isomers, it has been difficult to measure the coupling constants at less than 6.0 Hz. Dihedral angles calculated from the measured coupling constants are compared with those obtained by X-ray study in Table VI. The dihedral angles agree reasonably well, indicating that the conformations in solid state and solution (at least for the major isomer) are similar.

Acknowledgment. We thank the National Institutes of Health (Grant GM32690) for financial help.

Supplementary Material Available: Bond lengths and angles (Table VII), hydrogen atom positions (Table VIII), and anisotropic thermal parameters (Table IX) for halomycin B (7 pages). Ordering information is given on any current masthead page.